

CRYSTAL CHEMISTRY OF THE ALLUAUDITE
STRUCTURE TYPE: CONTRIBUTION TO THE PARAGENESIS OF PEGMATITE PHOSPHATE GIANT CRYSTALS

PAUL B. MOORE, *Department of the Geophysical Sciences, The University of Chicago, Chicago, Illinois, 60637*

ABSTRACT

Three-dimensional crystal structure analysis of an alluaudite from the Buranga pegmatite, Central Africa, elucidated the crystal chemistry of the alluaudites (hagendorfite, hühnerkobelite, varulite, mangan-alluaudite, alluaudite, and the arsenate mineral caryinite). $R(hkl) = 0.09$ for 1250 symmetry independent reflections. The crystal parameters are a 12.004(2), b 12.533(4), c 6.404(1) Å, $\beta = 114.4(1)^\circ$, space group $C2/c$, cell contents approximately $\text{Na}_{2.5}\text{Li}_{0.1}\text{Ca}_{0.5}\text{Mn}^{2+}_{4.5}\text{Mg}_{0.2}\text{Fe}^{3+}_{7.9}(\text{PO}_4)_{12.0}$.

The alluaudite structure type involves four distinct larger cation coordination polyhedra, with mean M -O distances $X(1)$ -O 2.537, $X(2)$ -O 2.431 (four inner), 3.291 (six outer), $M(1)$ -O 2.206, and $M(2)$ -O 2.042 Å. The $X(1)$ -O polyhedron is a cube which shares faces with symmetry equivalent cubes forming chains which run parallel to $[001]$. In the Buranga sample, $X(2)$ is empty, but the inner coordination shell approximates a rhombus. The six-coordinated cation-oxygen polyhedra include $M(1)$ -O, a bifurcated tetragonal pyramid, and $M(2)$ -O, an octahedron. The proposed site occupancies in the cell are $X(1)$ 2.5 $\text{Na}^{1+} + 0.7 \text{Mn}^{2+} + 0.5 \text{Ca}^{2+} + 0.3 \square$, $X(2)$ \square , $M(1)$ 3.8 $\text{Mn}^{2+} + 0.1 \text{Mg}^{2+} + 0.1 \text{Li}^+$, and $M(2)$ 7.9 $\text{Fe}^{3+} + 0.1 \text{Mg}^{2+}$. The $M(1)$ - and $M(2)$ -O polyhedra share edges to form staggered chains which are stacked parallel to the $\{101\}$ plane. Equivalent chains are linked by $P(1)$ - and $P(2)$ -O tetrahedra to form pleated sheets oriented parallel to $\{010\}$. Symmetry equivalent sheets are held together by oxygen atoms associated with the $P(2)$ -O tetrahedra.

The present nomenclatures and paragenetic settings proposed for alluaudite are unfortunate and should be abandoned. Ideal end-member compositions for alluaudites are $\text{NaCaMn}^{2+}\text{Fe}^{2+}_2(\text{PO}_4)_3$ (unoxidized) and $\text{Mn}^{3+}\text{Fe}^{3+}_2(\text{PO}_4)_3$ (oxidized). Most natural samples involve mixed Fe valences and are derivative of the composition $\text{NaNaMn}^{2+}(\text{Fe}^{2+}\text{Fe}^{3+})(\text{PO}_4)_3$. Crystallochemical and field evidence suggest that alluaudites are derivative of triphylite, lithiophilite, ferri-sicklerite, and heterosite by Na-Li metasomatic exchange.

INTRODUCTION

The general study of transition metal phosphate crystal chemistry is an enormous problem. Only recently have detailed crystal structure analyses been directed toward some of the members of this richly populated but relatively rare family of minerals. Among the transition metal basic phosphate hydrates, no less than 40 species are known. Moore (1970a) has briefly outlined the chemistry of these "mineralogical step-children" as they are called by Fisher (1958) who lists 70 pegmatite phosphate species. Recently, Moore (1970b) has attempted to relate secondary Fe and Mn phosphate and arsenate hydrate crystal structures to their paragenetic settings on the basis of progressive condensation of the octahedral clusters with increasing temperature.

Nor does the knowledge of the primary phosphate crystal chemistry promise any easier road for the investigator. Fisher (1958) lists eight principal structure types of primary Fe-Mn phosphates. All occur as giant crystals from at least one locality. The *triphylites*—triphylite-lithiophilite, $\text{Li}(\text{Fe}, \text{Mn})^{2+}(\text{PO}_4)$ and the rare natrophilite, $\text{NaMn}(\text{PO}_4)$ —are based on the olivine structure type. Crystals of triphylite-lithiophilite are known to continuously pass into heterosite-purpurite, $(\text{Fe}, \text{Mn})^{2+}(\text{PO}_4)$ through transition metal oxidation and concomitant alkali-leaching. Giant crystals up to 10 feet across are known from the Palermo No. 1 pegmatite, North Groton, New Hampshire; several pegmatites in the Black Hills, South Dakota; Hagendorf Süd, Bavaria; and Varuträsk, Sweden. Refinement of the triphylite crystal structure has recently been published by Finger and Rapp (1970) who report ordered Li and Fe in the structure. *Griphite*, a problematical hydroxylated Ca, Na, Mn, Al phosphate, possibly a garnetoid (McConnell, 1942), occurs in abundance as ellipsoids of varying crystallinity at the Sitting Bull pegmatite, near Keystone, South Dakota (Roberts and Rapp, 1965). *Graftonite*, $\text{Ca}(\text{Fe}, \text{Mn}, \text{Ca})^{2+}_2(\text{PO}_4)_2$, occurs at many pegmatites as ellipsoidal masses, often showing laminated exsolution textures with *sarcopside*, $(\text{Fe}, \text{Mn}, \text{Mg})^{2+}_3(\text{PO}_4)_2$, and their crystal cell interrelationships have been described by Hurlbut (1965). The graftonite crystal structure was shown by Calvo (1968) to be isotypic to the $\text{CdZn}_2(\text{PO}_4)_2$ structure type, possessing three distinct larger cation coordination polyhedra: a trigonal bipyramid, a square pyramid and an irregular pentagonal bipyramid. The details of the sarcopside atomic arrangement are as yet unknown. The *triplite-zwieselite* pair, $(\text{Mn}, \text{Fe})^{2+}_2\text{F}(\text{PO}_4)$, are relatively rare primary phosphates with a structure based on chains of distorted Me-O octahedra, recently determined and described by Waldrop (1969). *Triploidite-wolfeite*, $(\text{Mn}, \text{Fe})^{2+}_2(\text{OH})(\text{PO}_4)$, are structurally related to triplite-zwieselite, but contain ordered $(\text{OH})^-$ anions instead of the disordered F^- anions, according to Waldrop.

This study concerns the Na-(Fe, Mn) phosphates of the *alluaudite* group of minerals. The other outstanding structure type involving Na and transition metal cations embraces the *dickinsonite-arrojadite* pair, $\text{Na}_2(\text{Mn}, \text{Fe})^{2+}_5(\text{PO}_4)_4(?)$ which possess a very complex crystal cell of unknown atomic arrangement. Recently alluaudite has received much attention and its presently documented localities are too numerous to list. Most noteworthy are several pegmatites in the Black Hills where the mineral occurs as large ellipsoidal masses of greenish-black color many pounds in weight. Its history has been fraught with controversy. Originally described by Damour (1848) from a locality in Chanteloube, France, the name was relegated to varietal status (under triphylite-

lithiophilite) by Dana (1920) until the investigation of Quensel (1937) on specimens from the Varuträsk pegmatite and further investigation on Chanteloube material by Mason (1940) suggested specific status for the mineral.

Fisher (1955) presented the first detailed crystal-chemical study on the alluaudite group of minerals and subsequently (Fisher, 1957) proposed the formula $W_{0-12}(X+Y)_{12}(PO_4)_{12}$, where $W = Na, Ca$; $X = Mn^{2+}, Fe^{2+}$; $Y = Fe^{3+}$. The naming of the end-member formulae is still a controversy. Fisher (1957) uses ferroan-alluaudite for Lindberg's (1950) hühnerkobelite from Norrö, Sweden; manganoan-alluaudite for the hagendorfite of Strunz (1954), the varulite and mangan-alluaudite of Quensel (1937); and ferrian-alluaudite for the hühnerkobelite described by Lindberg (1950) from Hühnerkobel, Bavaria. Palache, Berman, and Frondel (1951) define the series on the basis of $Fe^{2+}-Mn^{2+}-Fe^{3+}$ end-members with general composition $Na(A, B, C)(PO_4)$ with $A = Fe^{2+}$, $B = Mn^{2+}$, $C = Fe^{3+}$ as $A > B > C$ hühnerkobelite; $B > A > C$ varulite; $C > B > A$ alluaudite, and $B > C > A$ mangan-alluaudite. Strunz (1970) adopts a similar nomenclature but differentiates among large cation substitution for the general formula of Fisher with $Z = 4$, $W_{0-4}(X+Y)_3(PO_4)_3$. He distinguishes hagendorfite from hühnerkobelite where $W = Na > Ca$ for the former and $Ca > Na$ for the latter. Finally, I remark that caryinite, an arsenate containing Mn^{2+} , Mg^{2+} , Ca , Pb , and Na also belongs to the alluaudite structure type.

It is clear that alluaudite nomenclature has been confounded since no analysis of its atomic arrangement has appeared prior to the naming of the "end-members". On the basis of a detailed atomic arrangement study, I wish to demonstrate that all of the present nomenclatures are unfortunate and that the paragenetic history of the alluaudites needs re-interpretation.

EXPERIMENTAL

A superior single crystal of the Buranga pegmatite, Ruanda, Central Africa specimen described by Fisher (1955) was used in this study. Crystal cell computations based on the present structure analysis utilizing the accurate cell parameters of Fisher appear in Table 1. The crystal was a nearly perfect cube in outline, measuring 0.08 mm on an edge. It afforded 1800 symmetry independent reflections of the $k=0$ to 14 levels to $2\theta = 70^\circ$ with b as the rotation axis for PAILRED geometry and graphite monochromatized MoK_α radiation. The ω -rotations about the polar reflections indicated that absorption correction was not necessary, on account of favorable crystal shape, size, and composition. 1250 reflections were above background error and were the only ones used in subsequent study. With 2.0° half-angle scans, 20 second background counting times were taken on either side of the reflections. Coincidence of the peak maxima with the cell geometry of Fisher (1955) indicated that no re-examination of his crystal parameters was necessary. The data were processed to obtain $|F(obs)|$ through conventional computational procedures.

TABLE 1. ALLUAUDITE. CRYSTAL CELL CONTENTS¹

<u>a</u>	12.004 (2) Å
<u>b</u>	12.533 (4)
<u>c</u>	6.404 (1)
<u>β</u>	114.4 (1)
<u>space group</u>	C2/c
specific gravity	3.45
density (calc.) gm/cm ³	3.62
cell contents	Na _{2.5} Li _{0.1} Ca _{0.5} Mn _{4.5} ²⁺ Mg _{0.2} Fe _{7.9} ³⁺ (PO ₄) ₁₂

¹ Cell parameters and contents from Fisher (1955, 1965). The observed density is evidently low.

SOLUTION OF THE STRUCTURE

Single euhedral crystals of "hühnerkobelite" (Fe²⁺ > Fe³⁺; Mn²⁺) from the Palermo No. 1 pegmatite were goniometrically investigated by Moore (1965) and shown to be monoclinic holosymmetric, *2/m*. It was decided to attempt solution of the structure by direct methods using the IBM 7094 program MAGIC described by Dewar (1968). This program is based on the familiar symbolic addition procedure applied to normalized structure factors. A Wilson plot optionally built into the program revealed averages indicative of a non-centrosymmetric structure, *i.e.*, *Cc*, in contradiction with the morphological study of Moore (1965). Fortunately, it was decided to ignore the test for centrosymmetry on the basis of the normalized structure factors and the space group *C2/c* was assumed.

Despite the relatively small unit cell for alluaudite, solution of its structure proved most frustrating. One combination of five starting symbols resulted in sign determination of 400 of the strongest *E*'s with no apparent contradictions and revealed the four prominent densities whose coordinates are noted in Table 2. Parameter refinement converged to

$$R(hkl) = \frac{\sum |F(obs) - F(calc)|}{\sum |F(obs)|} = 0.34$$

for 1250 reflections. Despite such encouraging results, no sensible oxygen positions could be located on the subsequent Fourier map. After a sufficient amount of time was wasted on the problem, it was decided to prepare a three-dimensional Patterson function, $P(xyz)$. Sixteen prominent vectors appeared in the asymmetric unit, and all but two could be defined by the heavy atom model obtained from the E -map. It was noted that all sixteen prominent vectors could be located by a vector set analysis which shifted the initial atom parameters ($y+1/4$) for the $M(1)$ and $P(1)$ atoms situated on the two-fold rotor. This model converged to $R(hkl) = 0.26$ and is summarized in Table 2. Subsequent Fourier synthesis of the signs thus produced by the heavy atoms only revealed all six oxygen atoms in general positions in the asymmetric unit and additional density

TABLE 2. HEAVY ATOM COORDINATES FOR ALLUAUDITE.

	<u>MAGIC</u>	<u>3-D PATTERSON</u>	<u>FINAL LEAST SQUARES</u> ¹
<u>M(1)</u>	0	0	0
	0.011	0.260	0.260
	1/4	1/4	1/4
<u>P(1)</u>	0	0	0
	.471	-.280	-.286
	1/4	1/4	1/4
<u>M(2)</u>	.222	.229	.219
	.115	.155	.153
	.131	.130	.129
<u>P(2)</u>	.245	.229	.242
	-.153	-.120	-.109
	.134	.130	.132
<u>R(hkl)</u>	0.34	0.26	0.09

¹ Refinement includes oxygen atoms.

TABLE 3. ALLUAUDITE. CATIONIC CELL DISTRIBUTIONS, ATOMIC COORDINATES, AND ISOTROPIC TEMPERATURE FACTORS.

(Estimated standard errors in parentheses.)

		\bar{x}	\bar{y}	\bar{z}	$\bar{B}(\text{\AA}^2)$
$\bar{X}(1)$	$2.5\text{Na}^+ + 0.7\text{Mn}^{2+} + 0.5\text{Ca}^{2+} + 0.3\text{□}$	1/2	0	0	1.59 (14)
$\bar{X}(2)$	4 □	0	0	0	—
$\bar{M}(1)$	$3.8\text{Mn}^{2+} + 0.1\text{Mg}^{2+} + 0.1\text{Li}^+$	0	0.2599 (2)	1/4	.60 (3)
$\bar{M}(2)$	$7.9\text{Fe}^{3+} + 0.1\text{Mg}^{2+}$	0.2812 (1)	.6525 (1)	0.3713 (2)	.50 (2)
$\bar{P}(1)$	4.0P^{5+}	0	-.2855 (3)	1/4	.59 (5)
$\bar{P}(2)$	8.0P^{5+}	.2424 (2)	-.1089 (2)	.1325 (4)	.69 (4)
O(1)		.4533 (6)	.7152 (7)	.5342 (12)	.75 (10)
O(2)		.0988 (7)	.6375 (7)	.2401 (14)	1.22 (11)
O(3)		.3272 (7)	.6633 (7)	.1020 (13)	1.02 (10)
O(4)		.1213 (7)	.3974 (7)	.3119 (14)	1.41 (12)
O(5)		.2251 (7)	.8220 (7)	.3172 (13)	.92 (10)
O(6)		.3102 (7)	.5021 (7)	.3735 (14)	1.34 (12)

at 1/2, 0, 0. It is clear that the symbolic addition procedure worked in principle—the (x, z) coordinates of the incorrect and correct models are identical—but an apparent substructure is present resulting from the nearly identical (x, z) coordinates of the Fe, P pairs leading to ambiguities in the solution of the y -coordinates.

REFINEMENT

The free atomic parameters for the eleven independent atoms in the asymmetric unit were allowed to vary according to full-matrix least-squares refinement utilizing a local version of the ORFLS program for IBM 7094 computers by Busing, Martin, and Levy (1962). The scattering curve for the X(1) atom was obtained by averaging the values of $(2.5 \text{Na}^+ + 0.7 \text{Mn}^+ + 0.5 \text{Ca}^+)/4.0$. Scattering curves for Fe⁺, Mn⁺, Na⁺, Ca⁺, P³⁺, and O⁻ were obtained from the tabulations in MacGillavry and Rieck (1962). Final full-matrix atomic parameter and isotropic thermal vibration parameter refinements converged to $R(hkl) = 0.085$ for 957 reflections which were three times the mean background error and 0.098 for all 1250 reflections. The final atomic coordinates and isotropic thermal vibration parameters are listed in Table 3 and the $|F(\text{obs})| - F(\text{calc})$ data appear in Table 4.¹

¹ To obtain a copy of Table 4, order NAPS Document #01608 from National Auxiliary Publications Service of the A.S.I.S., c/o CCM Information Corporation, 866 Third Avenue, New York, New York 10022; remitting \$3.00 for microfiche or \$5.00 for photocopies payable, in advance, to CCMIC-NAPS.

DISCUSSION OF THE STRUCTURE

General Architecture. The alluaudite atomic arrangement is rather complex and is best examined in parts. The underlying motif is a chain of kinked and distorted octahedra which are stacked parallel to the $\{101\}$ plane. The $M(2)$ -O octahedral pairs join at an edge whose midpoint is the inversion center of $1/4, 1/4, 0$ etc. and these edge-sharing pairs link by sharing one edge apiece to a highly distorted six-coordinated $M(1)$ polyhedron at $0, y, 1/4$, etc. Members of the chain are linked by two oxygen atoms of the $P(1)$ -O tetrahedron with the remaining two oxygens linking to identical chains translated $(1+z)$ away. This results in a pleated sheet of tetrahedra and octahedra as shown in Figure 1a. Equivalent pleated sheets are generated by the 2_1 -screw operation. The $P(2)$ -O tetrahedron links two oxygen atoms to members of the chain, one to the equivalent chain translated $(1+z)$, and the remaining oxygen to the sheet related by the 2_1 -screw operation. Projected down the c^* -axis, it is seen that the individual chains form a corkscrew with relatively open spaces in between, at $y=0, 1/2$ (Fig. 1b).

Intercalated between the pleated sheets at $y=0$ and $1/2$ are the large cation polyhedra. The $X(1)$ polyhedron, partly occupied in Buranga alluaudite, is a distorted cube which shares faces with identical cubes to form chains running parallel to the c -axis. The cube is a sink for large cations such as Ca^{2+} and Na^+ , has point symmetry $\bar{1}$, and is situated at $1/2, 0, 0$ etc. Two pairs of the cubes' edges are shared by the $P(1)$ -O tetrahedron and the $M(1)$ -O polyhedron respectively. A remaining large cation site must be present in the alluaudite structure type to account for excess large cations revealed in the chemical analysis for most alluaudites discussed further on. Steric restrictions and known crystal-chemical stoichiometry require that the site be the remaining free inversion center at $0, 0, 0$ etc. It is highly irregular and consists of an inner coordination shell of four oxygen atoms defining a rhomb. This site, which is empty in Buranga alluaudite, is designated $X(2)$. A layer of $X(1)$ - and $X(2)$ -O polyhedra is shown in Figure 2. The alluaudite general crystallochemical formula is $4X(1) X(2) M(1) M(2)_2 (TO_4)_3$, where X are large cation polyhedral, M are distorted octahedral, and T the tetrahedral centers.

The atomic arrangement suggests that alluaudite has good $\{010\}$ and $\{\bar{1}01\}$ cleavages, which is entirely consistent with general observations on the Palermo crystals of Moore (1965) and the crystal cell study of Fisher (1955).

Despite the similarity in cell parameters, there does not appear to be any structural similarity with the garnet group. There is, however, a remote structural relationship with triplite, $(\text{Mn}, \text{Fe})_2\text{F}(\text{PO}_4)$, another phosphate occurring in a similar paragenesis. The alluaudite octahedral

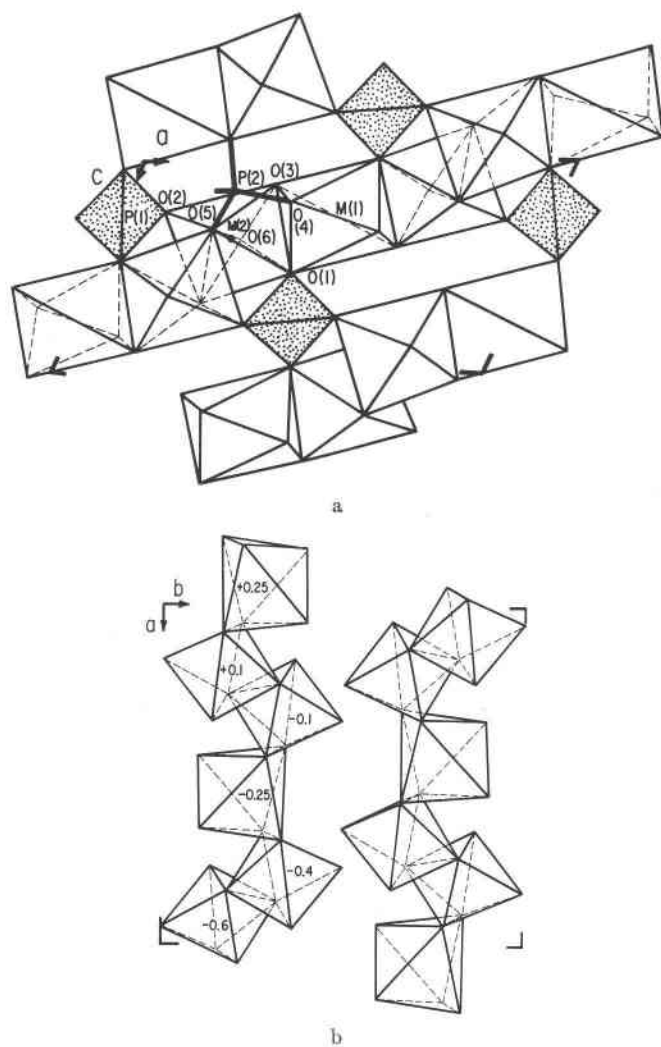


FIG. 1

chains can be topologically idealized as the staggered linear octahedral edge-sharing $M(1)-+2M(2)-O$ triplets featured in Figure 3 which is contrasted with the staggered edge-sharing $2M(1)-O$ doublets found in the triplite structure as determined by Waldrop (1969).

The Modular Units: Interatomic Distances. The individual $M-O$ and $X-O$ polyhedra differ considerably from each other; as a result, strong

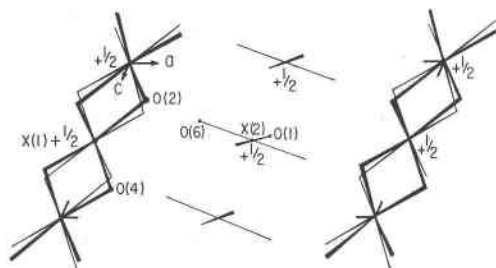


FIG. 2

ordering of cations with differing crystal radii over the available sites is expected. The $M(1)$ -O polyhedron, although topologically equivalent to an octahedron, structurally behaves more like a tetragonal pyramid with a split apex, that is, a bifurcated tetragonal pyramid. In fact, the polyhedron is so highly distorted that unusual polyhedral edge distances occur which cannot be reconciled with those of an octahedron whose distortions are explicable on the grounds of electrostatic arguments.

It is necessary to outline the crystal chemistry of the Buranga alluaudite. Based on 48 oxygen atoms, the calculation by Fisher reveals $\text{Na}_{2.51}\text{Ca}_{0.50}\text{Mn}^{2+}_{4.54}\text{Mg}_{0.23}\text{Li}_{0.12}\text{Fe}^{3+}_{7.86}\text{P}_{11.85}\text{O}_{48.00}$. The Buranga alluaudite represents a highly oxidized variety and possesses a favorable composition for assessing site preferences based on interatomic distances.

Polyhedral interatomic distances are listed in Table 5. The Me-O averages are $X(1)$ -O 2.54; $X(2)$ -O 2.43 (inner), 3.29 (outer); $M(1)$ -O 2.21; $M(2)$ -O 2.04; $P(1)$ -O 1.54; $P(2)$ -O 1.54 Å. Since the difference syn-

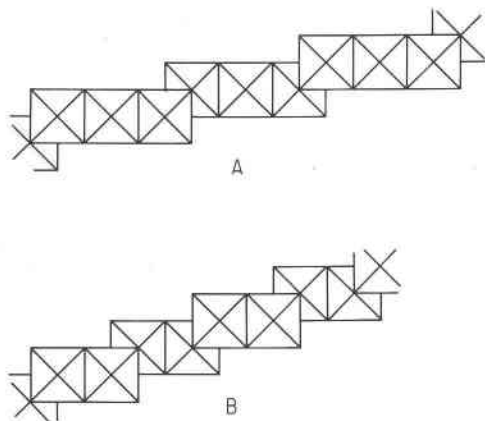


FIG. 3

TABLE 5. ALLUAUDITE. POLYHEDRAL INTERATOMIC DISTANCES¹.
 (Estimated standard errors: M-O, P-O, X-O+0.008 Å; Ø-O⁺+0.011 Å).

X(1)		M(1)		M(2)		P(2)	
2X(1)-O(2) ^{IV}	2.288	2M(1)-O(4)	2.184				
2 -O(4) ^I	2.315	2 -O(1) ¹¹	2.187	M(2)-O(6)	1.916	P(2)-O(6) ¹¹	1.522
2 -O(4) ¹¹¹	2.583	2 -O(3) ¹¹	<u>2.246</u>	-O(2)	2.004	-O(4) ¹¹	1.526
2 -O(2) ¹¹	<u>2.962</u>		2.206	-O(3)	2.021	-O(3) ^I	1.543
average	2.537 Å			-O(1)	2.048	-O(5)	<u>1.547</u>
				-O(5) ¹	2.052		1.535
20(2) ¹¹ -O(2) ^{IV}	2.427 ^{a,d}	20(3) ¹¹ -O(1) ¹¹	2.630 ^b				
20(4) ^I -O(4) ¹¹¹	2.684 ^{c,d}	20(4) ^I -O(4) ^V	2.684 ^c				
20(4) ^I -O(4) ¹¹¹	2.684 ^{c,d}	20(4)-O(3) ¹¹	3.002		2.042		
20(2) ^{IV} -O(4) ¹¹¹	2.898	20(4)-O(1) ¹¹	3.048				
40(2) ¹¹ -O(4) ¹¹	3.039 ^d	20(3) ¹¹ -O(1) ^{IV}	3.166	0(1)-O(3)	2.630 ^b	0(4) ¹¹ -O(5)	2.497
20(2) ¹¹ -O(4) ^I	<u>3.585</u>	20(4)-O(1) ^{IV}	<u>3.598</u>	0(2)-O(5)	2.697	0(3) ¹¹ -O(6) ¹¹	2.497
	2.945		3.038	0(1)-O(5) ¹	2.719	0(4) ¹¹ -O(6) ¹¹	2.506
				0(6)-O(3)	2.727	0(5)-O(6) ¹¹	2.518
				0(2)-O(5) ¹	2.796	0(3) ¹ -O(4) ¹¹	<u>2.520</u>
				0(5)-O(5) ¹	2.818 ^b		2.506
X(2)		P(1)					
inner:							
2X(2)-O(6) ¹¹	2.080	2P(1)-O(1) ¹¹¹	1.537	0(1)-O(5)	2.843		
2 -O(1) ¹¹	<u>2.782</u>	2P(1)-O(2)	<u>1.550</u>	0(2)-O(6)	2.874		
	2.431		1.544	0(3)-O(5)	2.958		
				0(5) ¹ -O(6)	3.107		
				0(1)-O(6)	3.112		
outer:							
2X(2)-O(3) ^I	3.168	10(2)-O(2) ^V	2.427 ^a	0(2)-O(3)	<u>3.226</u>		
2 -O(3) ¹¹	3.260	20(1) ¹¹¹ -O(2)	2.509				
2 -O(5)	<u>3.446</u>	10(1) ^I -O(1) ¹¹¹	2.518 ^c				
	3.291	20(2)-O(1) ^I	<u>2.576</u>				
			2.519				

¹The primed superscripts refer to the following transformations performed on the parameters in Table 2:
^I = 1/2-x, 1/2-y, -z; ¹¹ = 1/2-x, 1/2+y, 1/2-z; ¹¹¹ = 1/2+x, 1/2-y, 1/2+z; ^{IV} = 1/2+x, 1/2+y, z; ^V = -x, y, 1/2-z.

^aX(1)-P(1) shared edges

^bM(1)-M(2), M(2)-M(2)¹ shared edges

^cM(1)-X(1) shared edges

^dX(1)-X(1) shared edges

thesis showed that the X(2) site is empty, distribution of the larger cations must be over the X(1), M(1), and M(2) sites. The M(1)-O average distance is typical for Mn²⁺-O, that for M(2)-O is only slightly larger than the Fe³⁺-O averages found for many recently determined crystal structures. The eight-coordinated X(1) site affords an average in the range for larger cations such as Na⁺ and Ca²⁺. The most reasonable site distribution is M(1)=Mn²⁺, Li; M(2)=Fe³⁺, Mg; X(1)=Na, Ca. Discussion of the alluaudite composition is extended further on.

Electrostatic Valence Balances. The alluaudite interatomic distances combined with the predominant cations reported in chemical analyses suggest two ideal end-member formulae which are electrically balanced and it remains to demonstrate that the two models also conserve local charge

neutrality. The unoxidized end-member is $X(1)^{2+}_4X(2)^{1+}_4M(1)^{2+}_4M(2)^{2+}_8(PO_4)_{12}$, where $X(1)$ is predominantly Ca^{2+} , $X(2) = Na^{1+}$, $M(1) = Mn^{2+}$, and $M(2) = Fe^{2+}$, resulting in a composition for $Z=4$, $CaNaMn^{2+}Fe^{2+}_2(PO_4)_3$. The second model is its fully oxidized and alkali-leached equivalent, that is $X(1) = X(2) = \square$, $M(1) = Mn^{3+}$, $M(2) = Fe^{3+}$ or $Mn^{3+}Fe^{3+}_2(PO_4)_3$. Most alluaudite compositions as we shall see lie within these two compositional boundaries, disregarding substitutions of other cations of similar charge.

Table 6 presents electrostatic valence balance (Σ) calculations for the two end-member compositions. The unoxidized formula conserves local electrostatic neutrality with only slight deviations. The entire system is completely neutral if calculations are based only on the inner coordination shell about the $X(2)$ cation, suggesting to a first approximation that its coordination number is 4. In the fully oxidized hypothetical composition, individual anions are either electrostatically oversaturated or undersaturated with respect to the M -cations with a deviation $100 \times (\Sigma - 2.00) / 2.00 \sim 12$ percent in each case. This suggests that the oxidized equivalent is probably unstable as a primary crystallizing phase and that highly oxidized compositions such as found in the Buranga material reflect partial oxidation and alkali-leaching of the parent material after emplacement. The alluaudite structure type appears to be highly susceptible to partial oxidation, even more than the triphylite-lithiophilite group, since no unoxidized end-member compositions are

TABLE 6. ALLUAUDITE. ELECTROSTATIC VALENCE BALANCES (Σ) OF CATIONS ABOUT ANIONS.

		1	Σ	2	Σ
0(1)	$P(1) + M(1) + M(2) + X(2)$	$5/4 + 2/6 + 2/6 + 1/4$	2.16	$5/4 + 3/6 + 3/6$	2.25
0(2)	$P(1) + M(2) + 2X(1)$	$5/4 + 2/6 + 2/8 + 2/8$	2.08	$5/4 + 3/6$	1.75
0(3)	$P(2) + M(1) + M(2)$	$5/4 + 2/6 + 2/6$	1.92	$5/4 + 3/6 + 3/6$	2.25
0(4)	$P(2) + M(1) + 2X(1)$	$5/4 + 2/6 + 2/8 + 2/8$	2.08	$5/4 + 3/6$	1.75
0(5)	$P(2) + 2M(2)$	$5/4 + 2/6 + 2/6$	1.92	$5/4 + 3/6 + 3/6$	2.25
0(6)	$P(2) + M(2) + X(2)$	$5/4 + 2/6 + 1/4$	<u>1.84</u>	$5/4 + 3/6$	<u>1.75</u>
		sum	12.00		12.00

¹End-member composition $Na_4Ca_4Mn_4^{2+}Fe_8^{2+}(PO_4)_{12}$, where $X(1) = Ca$, $X(2) = Na$, $M(1) = Mn^{2+}$ and $M(2) = Fe^{2+}$.

²Oxidized equivalent: $X(1) = X(2) = \square$, $M(1) = Mn^{3+}$, $M(2) = Fe^{3+}$.

known. On the other hand, the completely oxidized equivalent— $M^{3+}(PO_4)$ —has not yet been documented. Partial oxidation may result from the relative ease of leaching the $X(2)$ cations and the likely primary co-crystallization of both Fe^{2+} and Fe^{3+} cations in the $M(2)$ position. The latter point will be advanced as a key in the paragenesis of primary alluaudites. It is believed that an important contribution to mixed Fe valences results from the predominance of Na^+ over *both* X -positions for most analyzed alluaudites and the necessity for some M -cations of higher valence than $2+$.

It now remains to explain the interatomic distances in Table 5 on the basis of the electrostatic valence balances and polyhedral edge- and face-sharing. $O(6)$, for both hypothetical end-members, is undersaturated with $\Sigma=1.84$ and 1.75 for the unoxidized and oxidized compositions. Accordingly, its distances, $M(2)-O(6)$ 1.92, $P(2)-O(6)$ 1.52, $X(2)-O(6)$ 2.08 Å are the shortest for their polyhedra. Four kinds of shared edges are present. In order of predicted decreasing cation-cation repulsion effects across the edges, they are $X(1)=O=P(1)$; $M(1)=O=M(2)$, $M(2)=O=M(2)$; $X(1)=O=M(1)$; and $X(1)=O=X(1)$. Since Table 5 lists interatomic $O-O'$ distances in increasing value, shared edge distances approximately follow the order of cation-cation repulsions in the tabulation. That is, they occur toward the top of the list. Adherence to the electrostatic model adds further confidence to the crystal-chemical interpretations of alluaudite compositions discussed further on.

Summing up, I conclude that the alluaudite structure is particularly favorable for a proposed cation ordering scheme which can be stated with some confidence. In particular, (1) two end-member formulae can be written, representing the unoxidized and oxidized compositions, and (2) the four non-equivalent larger cation sites $X(2)$, $X(1)$, $M(1)$, and $M(2)$ differ considerably from each other in shape and size, with decreasing $Me-O$ average distances $X(2) \gg X(1) \gg M(1) > M(2)$.

CRYSTAL CHEMISTRY OF THE ALLUAUDITES

Good fortune has blessed mineralogy with an abundance of alluaudite chemical analyses. Fisher (1965), in his definitive work on dickinsonites, fillowites, and alluaudites, compiled 11 separate alluaudite unit cell computations based on 48 oxygen atoms. This is fortunate since the compilation can be directly applied to the present study. In that paper, Fisher proposes the formula $W_{4-8}(X+Y)_{12}(PO_4)_{12}$, where $W = Na + Ca + K + Mn$ (in some cases); $X = Mn + Fe^{2+} + Mg + Li + Ca$ (in some cases), $Y = Fe^{3+}$. The upper limit of W is the limiting crystal-chemical formula proposed earlier: $X(1)_4X(2)_4M(1)_4M(2)_8(PO_4)_{12}$. Thus, $(X(1)+X(2)) = W$ and $(M(1)+M(2)) = (X+Y)$. The order of increasing expected

crystal radius for cations recorded in alluaudite analyses is $\text{Fe}^{3+} < \text{Mg}^{2+} < \text{Li}^+ < \text{Fe}^{2+} < \text{Mn}^{2+} < \text{Ca}^{2+} < \text{Na}^+ < \text{K}^+$. From the preceding discussion on the polyhedra in alluaudite, the smallest cations should occupy $M(2)$, followed by $M(1)$, $X(1)$, and $X(2)$ in that order.

Accordingly, the 11 cell computations of Fisher were rewritten on the basis of placing smallest cations first in $M(2)$, then $M(1)$, and so on. The results appear in Table 7. They indicate a distinct departure from all proposed alluaudite nomenclatures. Particularly interesting is the predominance of Mn^{2+} in all $M(1)$ sites except for the Norrö sample, but even here the distribution is nearly equally divided between Mn^{2+} and Fe^{2+} . Furthermore, it is not known for certain just how much reliability can be placed on the analyses since contamination, especially from triphylites and heterosites is always present in partly oxidized alluaudite nodules. Suffice it to say that Mn^{2+} plays an important structural role in alluaudites and may result from the unusual shape of the $M(1)$ -O polyhedron.

Disregarding the distinction between the X -cations it is evident that all alluaudites fall into the series $\text{NaCaMn}^{2+}\text{Fe}^{3+}_2(\text{PO}_4)_3\text{-Mn}^{3+}\text{Fe}^{3+}_2(\text{PO}_4)_3$. Distinguishing the X -cations however leads to an important addition to the series since sodium tends to be the predominant X -cation in most alluaudites. It may be written $\text{Na}^{1+}\text{Na}^{1+}\text{Mn}^{2+}(\text{Fe}^{2+}\text{Fe}^{3+})(\text{PO}_4)_3$. This implies the following coupled relationships:

	$X(2)$	$X(1)$	implies	$M(2) \rightleftharpoons M(2)'$	
1.	Na^+	Ca^{2+}	implies	$(\text{Fe}, \text{Mn})^{2+}$	$(\text{Fe}, \text{Mn})^{2+}$
2.	Na^+	Na^+	implies	$(\text{Fe}, \text{Mn})^{2+}$	Fe^{3+}
3.	\square	Na^+	implies	Fe^{3+}	Fe^{3+}

All alluaudites (with the possible exception of the Norrö sample, because of predominant Fe^{2+} in the $M(1)$ position) can be referred to these ideal compositions. The combination in (2) is the most persistent in the analyses, suggesting that most alluaudites crystallize as primary phases with mixed (Fe^{2+} , Fe^{3+}) valences in the $M(2)$ position. This conclusion is evident, solely from charge balances, even though most alluaudites probably have been further oxidized after primary emplacement. Since the $M(2)$ -O octahedra share a common edge pairwise, mixed valence homonuclear electron transfer would result in the characteristic deep green color generally observed for the alluaudites. The persistent mixed (Fe^{2+} , Fe^{3+}) valence states in alluaudite are distinct from the primary phosphates in the triphylite-lithiophilite, triplite and arrojadite-dickinsonite groups which do not appear to possess mixed Fe^{2+} , Fe^{3+} valence states when crystallized as primary phases.

Re-examination of the existing nomenclatures for alluaudite reveals

TABLE 7. PROPOSED SITE DISTRIBUTIONS FOR ALLHAUDITES AND CARYINITE¹

	$\bar{M}(2)$	$\bar{M}(1)$	$\bar{X}(1)$	$\bar{X}(2)$
Skumpetoxp	$1.6\text{Fe}^{3+} + 3.4\text{Fe}^{2+} + 3.0\text{Mn}^{2+}$	$3.10\text{Mn}^{2+} + 1.0\text{Ca}$	$0.3\text{Ca} + 3.7\text{Na}$	$2.6\text{Na} + 1.4 \square$
Varutråsk (2)	$1.9\text{Fe}^{3+} + 1.2\text{Li} + 2.8\text{Fe}^{2+} + 2.1\text{Mn}^{2+}$	4.0Mn^{2+}	$1.0\text{Mn}^{2+} + 0.9\text{Ca} + 2.1\text{Na}$	$3.3\text{Na} + 0.7 \square$
Lemmås	$3.3\text{Fe}^{3+} + 0.3\text{Mg} + 0.6\text{Fe}^{2+} + 3.8\text{Mn}^{2+}$	4.0Mn^{2+}	$0.2\text{Mn}^{2+} + 1.7\text{Ca} + 2.1\text{Na}$	$3.8\text{Na} + 0.2\text{K} \square$
Hagedorf	$3.3\text{Fe}^{3+} + 1.3\text{Mg} + 0.3\text{Li} + 2.8\text{Fe}^{2+}$	4.0Mn^{2+}	$1.1\text{Mn}^{2+} + 0.6\text{Ca} + 2.3\text{Na}$	$3.2\text{Na} + 0.1\text{K} + 0.7 \square$
Norrvå	$4.2\text{Fe}^{3+} + 0.4\text{Li} + 0.6\text{Fe}^{2+} + 2.8\text{Mn}^{2+}$	$2.3\text{Fe}^{2+} + 1.7\text{Mn}^{2+}$	$1.1\text{Mn}^{2+} + 0.5\text{Ca} + 2.4\text{Na}$	$3.9\text{Na} + 0.1 \square$
Varutråsk (1)	$5.1\text{Fe}^{3+} + 0.1\text{Li} + 1.0\text{Fe}^{2+} + 1.8\text{Mn}^{2+}$	4.0Mn^{2+}	$0.7\text{Mn}^{2+} + 0.8\text{Ca} + 3.5\text{Na}$	$1.0\text{Na} + 3.0 \square$
Sukula	$6.5\text{Fe}^{3+} + 2.5\text{Mn}^{2+}$	4.0Mn^{2+}	$1.0\text{Ca} + 3.0\text{Na}$	$2.3\text{Na} + 1.7 \square$
Chanteloube	$6.8\text{Fe}^{3+} + 0.5\text{Li} + 0.4\text{Mg} + 0.3\text{Fe}^{2+}$	$1.7\text{Fe}^{2+} + 1.9\text{Mn}^{2+} + 0.4\text{Ca}$	$0.4\text{Mn}^{2+} + 0.6\text{Ca} + 2.5\text{Na} + 0.5 \square$	\square
Hühnerkobel	$7.6\text{Fe}^{3+} + 0.2\text{Li} + 0.2\text{Fe}^{2+}$	$0.2\text{Fe}^{2+} + 3.6\text{Mn}^{2+} + 0.2\text{Ca}$	$3.2\text{Ca} + 0.8\text{Na}$	$1.7\text{Na} + 2.3 \square$
Pringle	$7.9\text{Fe}^{3+} + 0.1\text{Mg}$	$0.1\text{Mg} + 0.1\text{Li} + 3.8\text{Mn}^{2+}$	$1.2\text{Ca} + 2.8\text{Na}$	\square
Burenga			$0.7\text{Mn}^{2+} + 0.5\text{Ca} + 2.5\text{Na} + 0.3 \square$	\square
Långban (caryinite)	$2.0\text{Mg} + 0.2\text{Fe}^{2+} + 5.8\text{Mn}^{2+}$	$1.1\text{Mn}^{2+} + 2.9\text{Ca}$	$2.8\text{Ca} + 1.2\text{Pb}$	4.0Na ($0.4\text{Na} + 0.2\text{K}$)

¹ Locations refer to cell calculations of Fisher (1965). The major site constituent is underlined.

that ambiguities abound. Table 8 lists the ideal site populations in excess of 50 atomic percent, each of which is technically capable of an end-member name. Corresponding to these compositions are the distributions of Table 7 which best fit the respective end-member composition. Because of the coupled relationship between $X(2)+X(1)$ and $2M(2)$, no simple and unambiguous nomenclature is possible, especially when substituting cations of different valence (such as Li^+) are present in the M -sites.

All present nomenclatures are ambiguous; it would be sheer pedantry to name *all* corresponding end-member compositions. Besides, it is questionable whether many of the compositions can be defined without recourse to crystal structure analysis. I propose that all specific names be

TABLE 8. ALLUAUDITE: POSSIBLE END-MEMBERS.

$X(2)$	$X(1)$	$M(1)$	$M(2)$	
Na	Ca	Mn^{2+}	$Fe^{2+} > Mn^{2+}$	Hagendorf?, Varutrask (2)?, Skrupetorp
Na	Ca	Mn^{2+}	$Mn^{2+} > Fe^{2+}$	Lemnas
Na	Ca	Fe^{2+}	Fe^{2+}	
Na	Na	Mn^{2+}	$Fe^{3+} > Mn^{2+}, Fe^{2+}$	Sukula
Na	Na	Fe^{2+}	$Fe^{3+} > Fe^{2+}$	Norrö
□	Ca	Mn^{2+}	$Fe^{3+} > Fe^{2+}, Mn^{2+}$	Hühnerkobel
□	Ca	Fe^{2+}	$Fe^{3+} > Fe^{2+}$	
□	Na	Mn^{2+}	Fe^{3+}	Buranga, Pringle, Chanteloube, Varutrask (1)
□	Na	Fe^{2+}	Fe^{3+}	
□	□	Mn^{3+}	Fe^{3+}	
□	□	Fe^{3+}	Fe^{3+}	

abandoned except the one name with priority—alluaudite. This name shall include the structure type embracing the compositions found in pegmatitic phosphates. Modifiers, specifying the cations and oxidation states present, should be used in accordance with the guidelines set down by the International Commission on New Mineral Names. In any event, the nomenclatures as they now exist in the literature, are without logical foundation.

Caryinite has been suggested by Strunz (1960) to belong to the alluaudite structure type. Boström (1957) noted a few very weak reflections on single crystal photographs of type caryinite which violated the space group $C2/c$, suggesting $P2_1/c$ instead. However, the similarity in cell parameters between caryinite and alluaudite leaves little doubt that the compounds are closely related structurally. The suggested caryinite cationic distribution in Table 7 based on the analysis of Mauzelius in Boström (1957) is $(Na)(Ca, Pb)(Ca, Mn)(Mn, Mg)_2(AsO_4)_3$ or $NaCa_2Mn_2(AsO_4)_3$.

The present analysis and interpretation of alluaudites indicate that at least two important features contribute to the alluaudite paragenesis. Summed up, they are (1) Mn^{2+} is an essential constituent of alluaudites, occurring in the $M(1)$ position, and (2) all published compositions require that some iron must be present in the trivalent state during emplacement. This second observation distinguishes alluaudite from the other primary Fe-phosphates.

THE ALLUAUDITE PARAGENESIS

It is generally accepted that a parallel progressive oxidation and alkali-leaching exists for the primary phases alluaudite and triphylite-lithiophilite and that the final fully oxidized and alkali-leached products are heterosite-purpurite. This contention is a result of an extensive and noteworthy study on the iron-manganese phosphates by Mason (1941). The evidence that triphylite progressively oxidizes through a sequence which concludes with heterosite is indisputable and commonly observed in Nature. A key feature of this progressive process of oxidation and alkali-leaching is the retention of the olivine structure type. It is also pertinent to note that heterosite-purpurite does not occur as a primary phase nor has its synthesis been achieved. This suggests that heterosite-purpurite is probably unstable and is derived only from parent triphylite-lithiophilite.

Since the alluaudite structure type is not even remotely related to that of triphylite, it is difficult to accept heterosite-purpurite as a final oxidation product, since a gross reconstructive reaction would have to take place. This structural change would have to occur only at the final stages of alkali-leaching, that is, beyond the composition $Na^+Mn^{2+}Fe^{3+}_2(PO_4)_3$. Since such a reaction is unlikely, an alternative explanation seems necessary. The alluaudite \rightarrow heterosite sequence, although hypothetically advanced by Quensel (1937), rests on several observations by Mason (1941):

“During this investigation I took powder photographs of authentic Na-purpurite occurring together with the alluaudite from central France. These photographs were identical with powder photographs of heterosite and purpurite derived from triphylite and lithiophilite. Powder photographs of authentic Na-purpurite from Varuträsk were also identical with powder photographs of the ordinary heterosite and purpurite.”

Mason (1941) successfully interpreted and duplicated the complex Na-purpurite powder pattern of Björling and Westgren (1938) as a mechanical mixture of alluaudite and purpurite, adding seemingly further evidence to the alluaudite \rightarrow heterosite degradation.

I question the generally accepted conclusion that heterosite is even a possible product of alluaudite, and submit a remarkable specimen as

evidence to the contrary. A section of an ellipsoidal "log" of heterosite measuring six inches along its major axis (specimen No. 40, collected by D. J. Fisher from the Green pegmatite, Pringle, South Dakota in 1942) was sawn in half. The log, apparently a corroded single crystal of parent triphylite, showed numerous fractures filled with quartz.

Four distinct phases are present and were identified by X-ray powder diffraction. Fracture fillings of quartz (grey), deposited by solutions which invaded the fractured parent material, course through the phosphate log. Immediately in contact with the quartz is the olive-green mineral which proved to be the alluaudite. The alluaudite everywhere surrounds and replaces the brown ferri-sicklerite and the purple heterosite.

The sample leaves little doubt that metasomatic exchange took place during oxidation and alkali-leaching of the parent triphylite log. Removed from the triphylite parent was Li^+ while Na^+ was later added, resulting in an aureole of alluaudite surrounding ferri-sicklerite and heterosite. Indeed, the process of metasomatic exchange of Na^+ for Li^+ (or for vacancies in the heterosite) results in a paragenesis exactly the reverse of that proposed by Mason (1941).

Another interesting specimen consists of a cross-section of a euhedral triphylite crystal, completely oxidized to heterosite. I collected this sample from the Rock Ridge pegmatite, near Custer, South Dakota. The cross-section shows the deep purple heterosite laced with fractures and crenulations which show dull olive-green alluaudite replacing the heterosite. A third specimen, collected by D. J. Fisher from the Pleasant Valley pegmatite near Custer, South Dakota shows alluaudite with a dendritic pattern replacing the heterosite. The "dendrite" arms represent the trace of the heterosite perfect cleavage planes. Again the alluaudite postdates the heterosite.

Several other nodules of alluaudite-heterosite were examined. In particular slabs of the nodules described by Roberts and Rapp (1965) as ". . . alluaudite partly altered to heterosite . . ." reveal that exactly the reverse is true in each instance; alluaudite metasomatically replaces the heterosite. I propose that Mason's (1941) samples were in fact mixtures of alluaudite and heterosite in a similar paragenesis.

Is there evidence that alluaudite actually crystallizes as a primary pegmatite giant crystal phase or are alluaudites the products of Na-metasomatism of triphylite? Moore (1965) has described euhedral "hühnerkobelite" crystals but they probably formed at a much later stage than the alluaudite nodules. Where total exchange of alluaudite for triphylite took place, it would be difficult to distinguish a metasomatic process from primary crystallization. However, the generally rude out-

line of the alluaudite ellipsoids, contrasted with the frequent subhedral to euhedral character of triphylite crystals; the fine-grained nature of the alluaudite nodules, usually showing lack of broad cleavage surfaces; and the prevalence of quartz-filled networks through alluaudite nodules where absence of such is the rule in fresh triphylites—all suggest that Na-metasomatism is an important mechanism in the formation of at least some, if not all, alluaudite nodules. Strunz (1954) observed that "hagendorfite" occurs later than triphylite and replaces it. Mason in Quensel (1956) placed alluaudite (varulite, etc.) after triphylite-lithiophilite, observing that the green mineral (= varulite) replaces the color-

TABLE 9. LOCATIONS AND PARAGENESES FOR ALLUAUDITE.
(fes=ferri-sicklevite; het=heterosite; ald=alluaudite - grain size in parentheses).

Location	Replaced mineral	Replacing mineral	Collector
Rock Ridge peg., S.D.	fes+het(1cm)	ald (0.2mm)	P.B. Moore
Pleasant Valley peg., S.D.	het (>1cm)	ald (0.1mm)	J. Norton
Greene peg., S.D.	fes+het (>1cm)	ald (0.2mm)	D.J. Fisher
Rainbow #4 peg., S.D.	fes+het (>1cm)	ald (0.5mm)	W.L. Roberts
Custer Mtn. lode, S.D.	lithiophilite (>1cm)	ald (0.1mm)	P.B. Moore
Ross lode, S.D.	fes (1cm)	ald (0.1mm)	P.B. Moore
Palermo #1, N.H.	ald (single xls, 1cm)	ludlamite (1mm)	P.B. Moore
Hagendorf, Bavaria	triphylite (>1cm)	ald ("hagendorfite") (>1cm)	H. Strunz
Norrö, Sweden	triphylite (>1cm)	ald ("hühnerkobelite")(0.1mm)	P.B. Moore
Alluaudite as the sole mineral, paragenesis uncertain:			
Rock Ridge peg., S.D.		>1cm	P.B. Moore
Helen mine, S.D.		0.2cm	D.J. Fisher
Dyke lode, S.D.		0.5mm	W.L. Roberts
Townsite lode, S.D.		0.5mm	W.L. Roberts
Skrumpetorp, Sweden		0.1mm	P. Quensel

less mineral (= lithiophilite) from Varuträsk. Mason (1942) earlier observed "arrojadite" (= alluaudite) replacing triphylite from Hühnerkobel, Bavaria. Lindberg (1950), amplifying this point, noted that the "hühnerkobelite" from Hühnerkobel and Norrö, are associated with triphylite. I have personally examined specimens from all these localities and concur with the other investigators, that alluaudites replace the triphylites. There remains little doubt that alluaudites are metasomatic products of the triphylites-heterosites and have been derived at nearly all stages of triphylite oxidation.

Table 9 is a list of all alluaudite locations where I have personally inspected sawn sections of collected nodules. In general, the grain size of the alluaudite is an order of magnitude smaller than the mineral which it replaces. The only indisputable observation of alluaudite as

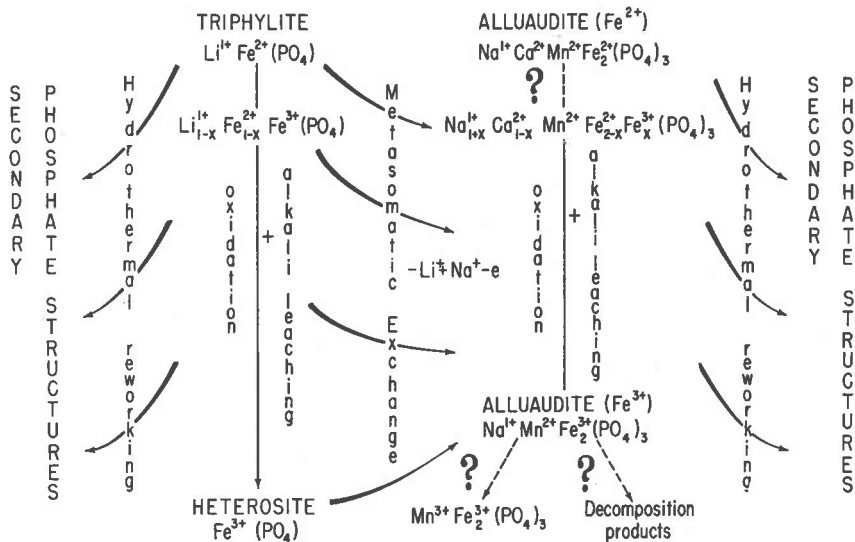


FIG. 4

euohedral single crystals is that from the Palermo No. 1 pegmatite. Here, the crystals are partially replaced by ludlamite, indicative of a hydrothermal reworking which results in species similar to the reworking of triphylite. Summing up, alluaudites have been observed to replace triphylite, lithiophilite, ferri-sicklerite, heterosite and presumably their Mn^{3+} -rich members.

With the observations offered here and the conclusions reached, I propose a paragenetic tree for triphylite and alluaudite in Figure 4. Although it is not clear what the final oxidation product of alluaudite is, the heterosite-alluaudite branch is connected in one direction, that is alluaudite replaces heterosite. In the field, alluaudites (at least in the final stages of oxidation) appear to be more resistant to total oxidation than triphylites. Perhaps this is the consequence of the proposed independent role of Mn^{2+} in the $M(1)$ site of alluaudites—or that alluaudites decompose to oxyhydroxide nodules at the final stage instead of $\text{M}^{3+}(\text{PO}_4)$. More evidence is needed to establish this portion of the tree.

ACKNOWLEDGEMENTS

Without important samples, the paragenetic study would have been impossible. Dr. David H. Garske supplied the specimens described by Roberts and Rapp (1965) and Professor D. Jerome Fisher provided samples used in his studies. I thank Eman. Lars Tallbacka who arranged for my visit to the Norrö pegmatite in 1968.

This study was supported by a Dreyfus Foundation award and the N.S.F. GA10932 grant.

REFERENCES

- BJÖRLING, C. O., AND A. WESTGREN (1938) Minerals of the Varuträsk pegmatite. IX. X-ray studies on triphylite, varulite and their oxidation products. *Geol. Fören. Stockh. Förhandl.* **60**, 67-72.
- BOSTRÖM, K. (1957) The chemical composition and symmetry of caryinite. *Ark. Mineral. Geol.* **2**, 333-336.
- BUSING, W. R., K. O. MARTIN, AND H. A. LEVY (1962) ORFLS, a Fortran crystallographic least-squares program. *U.S. Oak Ridge Nat. Lab. (U.S. Clearinghouse Fed. Sci. Tech. Info.) Rep. ORNL-TM-305*.
- CALVO, C. (1968) The crystal structure of graftonite. *Amer. Mineral.* **53**, 742-750.
- DAMOUR, M. A. (1848) Sur un nouveau phosphate de fer, de manganèse et de soude, l'*Alluaudite*, trouvé dans le département de la Haute-Vienne. *Ann. Mines* **13**, Ser. 4, 341-350.
- DANA, E. S. (1920) *The System of Mineralogy of J. D. Dana, 6th ed.* John Wiley and Sons, Inc., New York, 757.
- DEWAR, R. B. K. (1968) *Use of Computers in the X-ray Phase Problem*. Ph.D. Dissertation, Univ. Chicago (Dept. Chemistry), Chicago, Ill., p. 16-101.
- FINGER, L. W. AND G. R. RAPP, JR. (1970) Refinement of the crystal structure of triphylite. *Carnegie Inst., Wash. Year Book* **69**, 290-292.
- FISHER, D. J. (1955) Alluaudite. *Amer. Mineral.* **40**, 1100-1109.
- (1957) Alluaudites and varulites. *Amer. Mineral.* **42**, 661-664.
- (1958) Pegmatite phosphates and their problems. *Amer. Mineral.* **43**, 181-207.
- (1965) Dickinsonites, fillopite, and alluaudites. *Amer. Mineral.* **50**, 1647-1669.
- HURLBUT, C. S., JR. (1965) Detailed description of sarcopside from East Alstead, New Hampshire. *Amer. Mineral.* **50**, 1698-1707.
- LINDBERG, M. L. (1950) Arrojadite, hühnerkobelite and graftonite. *Amer. Mineral.* **35**, 59-76.
- MACGILLAVRY, C. H., AND G. D. RIECK (1962) *International Tables for X-ray Crystallography, Vol. 3*, The Kynoch Press, Birmingham, England.
- MASON, B. H. (1940) Triploidite and varulite from the pegmatite at Skruppetorp in Sweden. *Geol. Fören. Förhandl.* **62**, 373-379.
- (1941) Minerals of the Varuträsk pegmatite. XXIII. Some iron-manganese phosphate minerals and their alteration products, with special reference to material from Varuträsk. *Geol. Fören. Förhandl.* **63**, 117-175.
- (1942) Some iron-manganese phosphate minerals from the pegmatite at Hühnerkobel in Bavaria. *Geol. Fören. Stockh. Förhandl.* **64**, 335-340.
- MCCONNELL, D. (1942) Grīphite, a hydrophosphate garnetoid. *Amer. Mineral.* **27**, 452-461.
- MOORE, P. B. (1965) Hühnerkobelite crystals from the Palermo No. 1 pegmatite, North Groton, New Hampshire. *Amer. Mineral.* **50**, 713-717.
- (1970a) Crystal chemistry of the basic iron phosphates. *Amer. Mineral.* **55**, 135-169.
- (1970b) A crystal-chemical basis for short transition series orthophosphate and orthoarsenate parageneses. *Neues. Jahrb. Mineral. Monatsh.* **1970**, 39-44.
- PALACHE, C., H. BERMAN, AND C. FRONDEL (1951) *The System of Mineralogy . . . of Dana. Vol. 2* John Wiley and Sons, New York, 665-670.
- QUENSEL, P. (1937) Nya mineralfynd från Varuträsk pegmatiten. *Geol. Fören. Stockh. Förhandl.* **58**, 621.
- (1956) The paragenesis of the Varuträsk pegmatite. *Ark. Mineral. Geol.* **2**, 39-60.
- ROBERTS, W. L., AND G. RAPP, JR. (1965) Mineralogy of the Black Hills. *S. Dak. School Mines Technol. Bull. No. 18*, 8.

- STRUNZ, H. (1954) Hagendorfit, ein neues Mineral der Varulith-Hühnerkobelite Reihe. *Neues Jahrb. Mineral. Monatsh.* 1954, 252-255.
- (1960) Karyinit, ein Arsenat vom Struktur typus der Phosphate Hagendorfit und Alluaudit. *Neues Jahrb. Mineral. Monatsh.* 1960, 7-15.
- (1970) *Mineralogische Tabellen*, 5, Aufl. Akademische Verlagsgesellschaft, Geest und Portig K.-G., Leipzig, 310.
- WALDROP, L. (1969) The crystal structure of triplite, $(\text{Mn, Fe})_2\text{F}(\text{PO}_4)$. *Z. Kristallogr.* 130, 1-14

Manuscript received, April 8, 1971; accepted for publication, May 21, 1971.